euronoise

Exact solutions to the acoustic source reconstruction problem

Cédric Maury and Teresa Bravo

Université de Technologie de Compiègne, Centre de Recherche Royallieu, BP20529, 60205 Compiègne, France
cedric.maury@utc.fr

In this study analytical solutions are derived for the singular radiation and velocity patterns of a baffled elastic beam, thus leading to closed-form expressions for the singular value expansion of a number of integral operators which map a boundary velocity onto the acoustic pressure distribution radiated in far-field or intermediate regions. Exact solutions to this problem involve prolate spheroidal wave functions which correspond to a set of independent distributions with finite spatial support and with maximal energy concentration in a given bandwidth in the wavenumber domain. A stable solution to the inverse source reconstruction problem is obtained by decomposing the unknown boundary velocity into a number of efficiently radiating singular velocity patterns which corresponds to the number of degrees of freedom of the radiated field. It is found that the degree of ill-posedness of the inverse problem is significantly reduced when considering a hemi-circular observation arc with respect to a linear array of sensors, by a factor scaling on the small angular aperture subtended by the observation line. Estimates are derived of the spatial resolution limits that can be achieved in the source reconstruction problem from the dimension of the efficiently radiating subspace.

1 Introduction

A typical issue at the heart of the acoustic source identification problems is the reconstruction of a baffled planar velocity distribution from knowledge of the measured acoustic pressure radiated in free-field. In the Near-field Acoustical Holography (NAH), i.e. acoustic source reconstruction from near-field measurements, a stable and accurate approximation of the unknown source strength is numerically sought in terms of the Singular Value Decomposition (SVD) of the discretized forward operator which is an ill-posed linear compact operator. The SVD is a powerful tool which has been used in conjunction with regularization techniques to solve a number of NAH problems, for instance to provide IBEM (Inverse Boundary-Element Method) source reconstruction results robust to the presence of noise in the measured field data [1], to extract dominant acoustic modes in the Helmholtz Equation Least-Squares method [2] or to extend patch NAH to complex source geometries whilst avoiding the replication problem of the measurement window [3].

In the present study, closed-form expressions are found in terms of Prolate Spheroidal Wave Functions (PSWFs), when dealing with a model-based inverse approach, for the Singular Value Expansion (SVE) of the radiation kernel for a baffled beam or a baffled panel. Such analytical solutions solve a concentration problem, initially considered in the context of Communication Theory and Electrical Engineering by Slepian et al. [4], i.e. to find a class of finite support velocity patterns which encapsulate the largest fraction of energy in a given bandwidth in the wave-number domain. The theoretical framework developed provides a principled method of determining the number of independently-radiating velocity patterns required to obtain a stable reconstruction of the boundary velocity. In particular, it is shown how the analytical SVE of the radiation kernel allows to gain further insight into the nature of the singular pressure and velocity modes, the essential dimension of the radiating subspace, and the resolution properties of the reconstructed velocity distribution.

2 The acoustic source reconstruction problem

First, one considers the forward radiation problem illustrated in Fig. 1 in the two-dimensional case: a baffled elastic beam of length $2L'$, with a normal velocity distribution, $v(x')$, is harmonically excited and radiates into a fluid at rest. The radiated pressure is measured by a microphone at every point of an observation line (resp. arc) of extent $2L$ (resp. of radius $R = L$) located at a variable height (resp. radius) above the baffled beam.

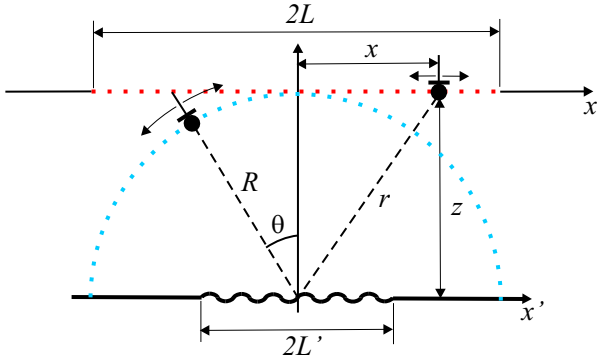

Figure 1. The vibrating beam and the observation points (line: red; arc: blue).

The radiated p pressure is expressed in terms of the boundary velocity v as

$$p(x,z) = \int_{-L'}^{L'} G^{+}(x-x',z)\,v(x')\,\mathrm{d}x', \qquad (1)$$

where G^{+} is the two-dimensional Green's function of the Helmholtz equation satisfying a Neumann boundary condition over the plane ($z = 0$). It reads $G^{+}(x-x',z) = \rho c k H_0^{(2)}(kr)/2$, where ρ is the fluid density, c is the sound speed, $k = \omega/c$ is the acoustic wavenumber and $H_0^{(2)}$ is the Hankel function of second kind and zero order. Assuming $z >> L + L'$, the pressure radiated in the intermediate (or pre-radiation) zone is expressed as a spatial finite Fresnel transform of the source distribution:

$$p(x,z) \approx \frac{\rho c}{\sqrt{\lambda z}}\, \mathrm{i}^{1/2} \mathrm{e}^{-\mathrm{i}kz} \int_{-L'}^{L'} \mathrm{e}^{-\mathrm{i}\pi(x-x')^2/(\lambda z)}\, v(x')\,\mathrm{d}x'. \qquad (2)$$

Furthermore, if $\lambda z >> \pi L'^2$, the pressure radiated on the far-field line is given in terms of the spatial finite Fourier transform, F_x, of the boundary velocity distribution, as follows

$$p(x,z) \approx \frac{\rho c}{\sqrt{\lambda z}} \mathrm{i}^{1/2} \mathrm{e}^{-\mathrm{i}kR} \mathrm{F}_x\{w_{L'} v\}(kx/z), \qquad (3)$$

Assuming $R >> L'$, the pressure radiated over the far-field observation arc is given by

$$p(R,\theta) \approx \frac{\rho c}{\sqrt{\lambda R}} \mathrm{i}^{1/2} \mathrm{e}^{-\mathrm{i}kR} \mathrm{F}_x\{w_{L'} v\}(k \sin\theta). \qquad (4)$$

A model-based approach requires the inversion of the radiation operators (2), (3) and (4) to retrieve the amplitude of the true velocity distribution v. These operators are associated to Fredholm linear integral equations of the first kind and their solutions are known to be ill-posed, i.e. to depend discontinuously on the measured data. Such ill-posed behaviour of the solution is all the more important that the observation domain is several wavelengths apart from the beam. In practice, there are often limiting factors such as acoustic diffraction effects on the sensors, signal distortion or harsh environments which limit the source-sensor separation distance to far-field or intermediate regions. A key point is then to determine the number of independent velocity source components that can be recovered accurately from band-limited pressure data acquired in these configurations.

3 Exact singular value expansion of the radiation operators

The problem is to find an exact decomposition of the radiation operators (2), (3) and (4) onto the corresponding sets of singular radiation and velocity patterns. The invariance properties satisfied by the PSWFs provide a solution to this problem since the radiation integral operators are directly related to the spatial finite Fourier (resp. Fresnel) transforms of the source velocity distribution, up to a scale and amplitude factor. Let R denote the far-field (resp. intermediate) radiation operators such that the boundary velocity v and its radiated field p satisfy $p = \mathrm{R}v$. The singular radiation and velocity patterns, respectively u_n and v_n, are solutions of $\mathrm{R}v_n = \sigma_n u_n$, with σ_n the corresponding singular value. The singular system of the far-field radiation operator (3) on the observation line is deduced from the self-reproducing property of the PSWFs after a scale change of variables. It is given by

$$\begin{cases} \sigma_n(\gamma_\mathrm{R}) = \dfrac{2\rho c}{\sqrt{\lambda z}} R_{0n}(\gamma_\mathrm{R}, 1), \\ u_n(\gamma_\mathrm{R}, x) = \mathrm{i}^{n+1/2} \mathrm{e}^{-\mathrm{i}k\sqrt{x^2+z^2}} \psi_n\left(\gamma_\mathrm{R}, \dfrac{x}{L}\right), \\ v_n(\gamma_\mathrm{R}, x') = \psi_n\left(\gamma_\mathrm{R}, \dfrac{x'}{L'}\right), \end{cases} \qquad (5)$$

where ψ_n is the nth normalised PSWF and $\gamma_\mathrm{R} = 2\pi LL'/\lambda z$ is the angular space-bandwidth parameter.

Simulations have been performed at 2 kHz assuming a baffled elastic beam of length $2L' = 4\lambda$ and rectilinear (resp. hemi-circular) observation domains of extent $2L = 8\lambda$ (resp. of radius $R = 100\lambda$). The acoustic transfer matrices are calculated between 81 evenly spaced observation points and 81 monopoles uniformly distributed over the beam length. Fig. 2 shows the exponential decay of the first singular values associated to the radiation operators (2-4) and determined from their analytic expressions. The values coincide with those computed from a SVD of the acoustic transfer matrix.

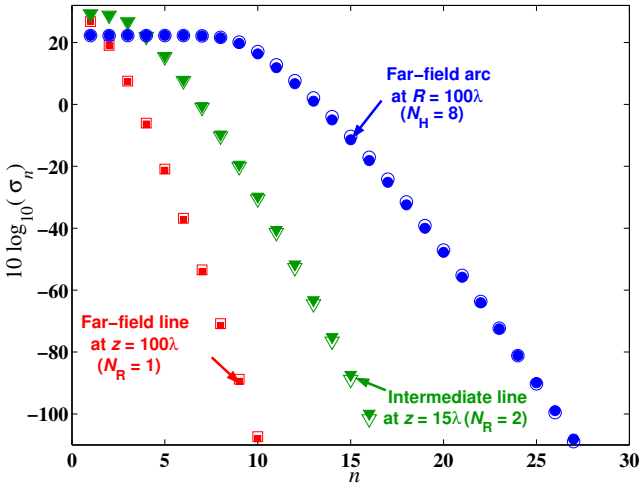

Fig. 2. The first singular values of the radiation operator which maps the source velocity onto a number of observation domains: far-field line (□, exact values; ■, SVD computation), far-field arc (○, exact values; ●, SVD computation), intermediate line (▽, exact values; ▼, SVD computation).

The singular system of the far-field radiation operator (4) on the observation arc is found to be

$$\begin{cases} \sigma_n(\gamma_\mathrm{H}) = \dfrac{2\rho c}{\sqrt{\lambda R}} R_{0n}(\gamma_\mathrm{H}, 1), \\ u_n(\gamma_\mathrm{H}, \theta) = \mathrm{i}^{n+1/2} \mathrm{e}^{-\mathrm{i}kR} \psi_n(\gamma_\mathrm{H}, \sin\theta), \\ v_n(\gamma_\mathrm{H}, x') = \psi_n\left(\gamma_\mathrm{H}, \dfrac{x'}{L'}\right), \end{cases} \qquad (6)$$

with $\gamma_\mathrm{H} = 2\pi L'/\lambda = kL'$. The singular velocity patterns v_n are the so-called "radiation modes", solutions of the eigenvalue problem, $\mathrm{R}^*\mathrm{R}v_n = \mu_n v_n = \sigma_n^2 v_n$, where R^* is the adjoint operator of R, which are known to maximise the radiation efficiency ratio μ_n of the radiator among all band-limited surface velocity distributions [5]. Figures 3(a-f) depict the beaming properties of the first six supersonic radiation patterns, as given by the expression (6) of u_n.

They closely agree with their numerical approximations, i.e. the left singular vectors of the acoustic transfer matrix. It can be seen from Fig. 3 that each supersonic radiation pattern beams in a particular direction within each quadrant with the least radiating modes beaming towards grazing angles from the source distribution. One infers that, for compact source distributions, it would be sufficient to use a hemi-circular array of microphones with an angular aperture limited to the largest beaming direction covered by the finite number of supersonic radiation patterns, as

determined by the angular space-bandwidth parameter γ_{H}. As expected, the number of secondary lobes increases as the radiation pattern order increases. It reflects the high spatial frequency content of the high order radiation patterns.

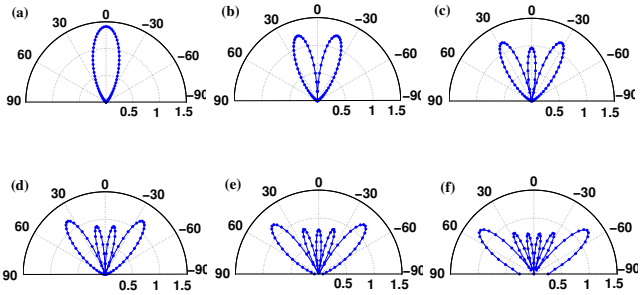

Fig. 3. Directivity diagrams of the first normalised singular radiation patterns associated to the far-field operator which maps the source velocity onto the hemi-circular observation arc: exact solution (curve) and SVD computation (*): u_0 (a), u_1 (b), u_2 (c), u_3 (d), u_4 (e), u_5 (f).

In the intermediate zone, the pressure radiated (2) is a finite Fresnel transform of the source velocity distribution, whose invariant forms are the converging PSWFs. It leads to the following singular system for the radiation operator in the intermediate region,

$$\begin{cases} \sigma_n(\gamma_{\mathrm{R}}) = \dfrac{2\rho c}{\sqrt{\lambda z}} R_{0n}(\gamma_{\mathrm{R}},1), \\ u_n(\gamma_{\mathrm{R}},x) = \mathrm{i}^{n+1/2}\mathrm{e}^{-\mathrm{i}kz}\mathrm{e}^{-\mathrm{i}\frac{\pi x^2}{\lambda z}}\psi_n\left(\gamma_{\mathrm{R}},\dfrac{x}{L}\right), \\ v_n(\gamma_{\mathrm{R}},x') = \mathrm{e}^{\mathrm{i}\frac{\pi x'^2}{\lambda z}}\psi_n\left(\gamma_{\mathrm{R}},\dfrac{x'}{L'}\right), \end{cases} \qquad (7)$$

with $\gamma_{\mathrm{R}} = 2\pi LL'/\lambda z$, the same angular space-bandwidth parameter as for the far-field rectilinear case.

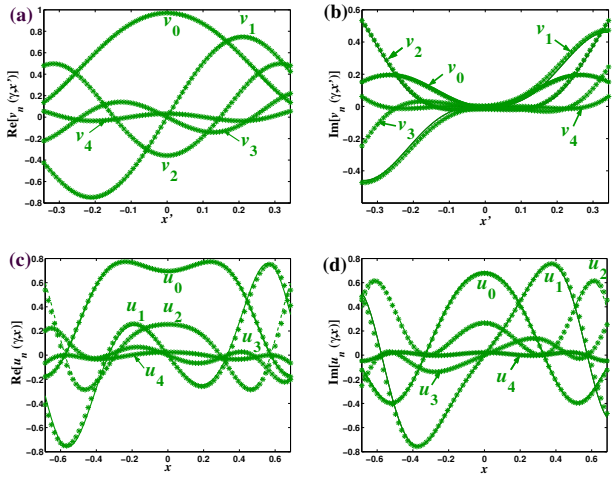

Fig. 4. The first normalised singular radiation and velocity patterns associated to the pre-radiation operator which maps the source velocity onto the observation line at $z = 15\lambda$ above the beam: exact solution (curve) and SVD (*) for $\mathrm{Re}[v_n]$ (a), $\mathrm{Im}[v_n]$ (b), $\mathrm{Re}[u_n]$ (c) and $\mathrm{Im}[u_n]$ (d).

Figure 4 shows that both the real and imaginary parts of the first five left and right singular vectors agree well with the exact values (7) of the corresponding singular velocity and radiation functions.

4 Accuracy of the reconstructed boundary velocity

A step-like distribution of the singular values associated to the far-field and intermediate radiation operators is shown in Fig. 2. Analytical expressions are obtained from Eqs. (5-7) for the number of Degrees Of Freedom (DOF) of the pressure field radiated over the far-field and intermediate lines, namely $N_{\mathrm{R}} = \lfloor 4LL'/\lambda z \rfloor$, and over the far-field hemi-circular arc, namely $N_{\mathrm{H}} = \lfloor 4L'/\lambda \rfloor$, where $\lfloor x \rfloor$ denotes the integer part of x. Hence, a regularization scheme based on the truncated singular value expansion of the operator appears to be well suited to provide a stable reconstruction of the boundary velocity from noisy pressure data. Let M be an appropriate truncation parameter. It corresponds to an "effective" number of DOFs, i.e. the minimum number of independent singular components required to represent the band-limited radiated pressure field in the presence of noise. It is a function of the Signal-to-Noise Ratio δ/σ, where δ is a given tolerance on errors in the reconstructed velocity and σ is the noise variance. It is given by:

$$M = \left\lfloor \frac{2kL'}{\pi}\sqrt{1+\frac{1}{(kz)^2}\mathrm{W}_0^2\left(kz\frac{\delta}{\sigma}\right)} \right\rfloor, \qquad (8)$$

where W_0 is the principal branch of the Lambert function W, which satisfies the functional equation $\mathrm{W}(u)\mathrm{e}^{\mathrm{W}(u)} = u$ and that takes real values for real $u \geq -\mathrm{e}^{-1}$ [6]. In particular, M is such that $\sigma_M \geq \sigma/\delta > \sigma_{M+1}$, so that one can only reconstruct the boundary velocity components for which the variance is greater than the variance in the reconstruction of the noise, σ^2/σ_n^2.

From Fig. 5, one observes that, for each type of observation domains, the spatial resolution of the reconstructed velocity improves as frequency increases, due to an increase with frequency of the number of DOF of the radiated field. Moreover, at any given frequency, Figs. 5(a) and 5(b) show that reconstruction from a hemi-circular arc of radius R enables to reveal far greater resolution information about the source distribution than reconstruction from a rectilinear array of quota, $z = R$, with a necessary limited aperture, $2L/z$. Fig. 5(c) shows the effect of noise contamination on the reconstruction of the piston-like boundary velocity. As the singular values decay exponentially beyond N_H, the essential dimension M of the radiation operator is at most equal to $N_H + 1$. In the simulations, the equality is reached with a SNR of 10^3. The presence of noise then leads to almost the same resolution as in the noise-free case, however at the expense of the accuracy in the

reconstruction, as it can be appreciated when comparing Figs. 5(b) and 5(c).

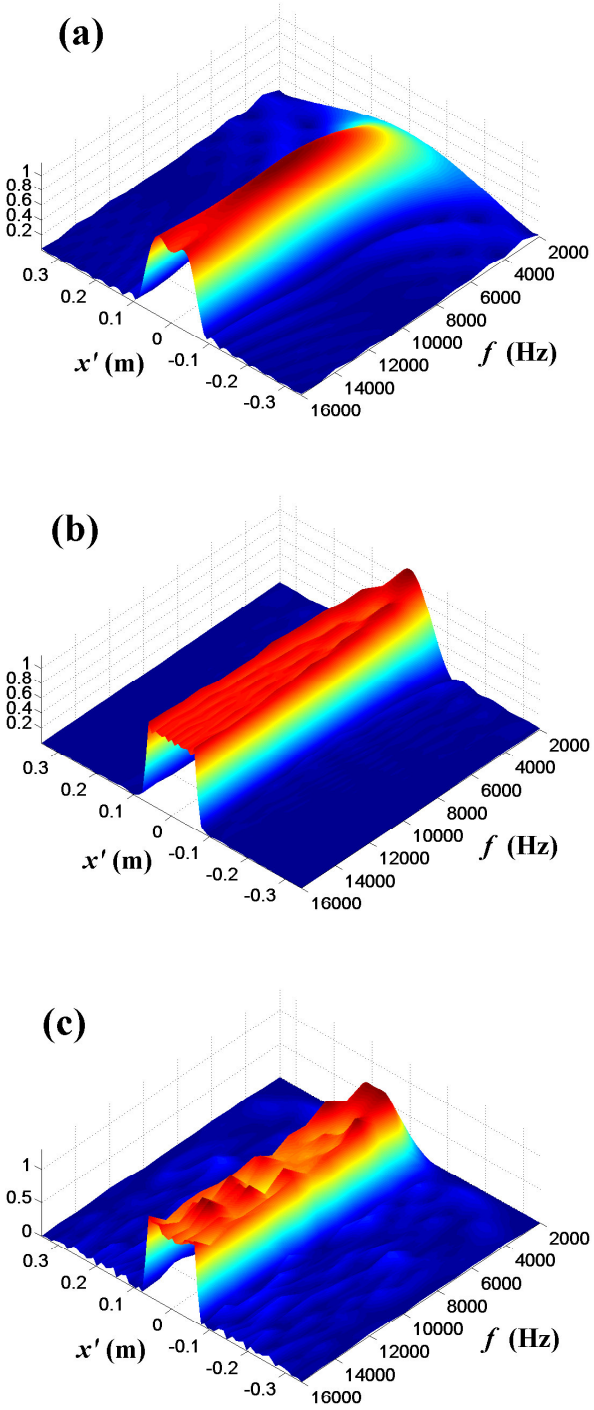

Fig. 5. Piston-like velocity distribution reconstructed from noise-free pressure data acquired over a far-field rectilinear (a) and a hemi-circular (b) observation domain and from noisy pressure data acquired over a far-field hemi-circular arc (c).

5 Conclusions

A formal analogy has been pointed out between the problem of determining the singular radiation and velocity patterns of a baffled planar vibrating structure and the invariance properties satisfied by the PSWFs under Fourier and Fresnel integral transforms. The closed-form expressions of the singular system are found to well correlate with the numerical solutions obtained from a SVD of the associated radiation matrices. A regularization scheme based on the truncated SVE is well-suited for source reconstruction from far-field or intermediate regions and a stable solution is found by decomposing the unknown boundary velocity into a finite number of efficiently radiating singular velocity patterns.

Acknowledgments

This research has been supported by the European Commission under the Sixth Framework program, contract INDUCT-MEIF-CT-2006-022579.

References

[1] A. Schuhmacher, J. Hald, K. B. Rasmussen, P. C. Hansen, "Sound source reconstruction using inverse boundary element calculations", *J. Acoust. Soc. Am.* 113, 114-127 (2003)

[2] Z. Wang, S. F. Wu, "Helmholtz equation least-squares (HELS) method for reconstructing the acoustic pressure field", *J. Acoust. Soc. Am.* 102, 2020-2032 (1997)

[3] E. G. Williams, *Fourier Acoustics: Sound Radiation and Nearfield Acoustical Holography*, 89-106, Academic Press, London, UK (1999).

[4] D. Slepian, H. O. Pollack, "Prolate spheroidal wave functions, Fourier analysis and uncertainty", I. *Bell Syst. Tech. J.* 40, 43-64 (1961).

[5] C. Maury, S. J. Elliott, "Analytic solutions of the radiation modes problem and the active control of sound power", *Proceedings of the Royal Society of London A* 461, 55-78 (2005)

[6] C. Maury, T. Bravo, "Analytic solutions to the acoustic source reconstruction problem", *Proceedings of the Royal Society of London A*, available on-line at http://dx.doi.org/10.1098/rspa.2007.0369 (2008).